*Quantum Electronics* **51** (11) 1004–1008 (2021) 

https://doi.org/10.1070/QEL17643

# Regime of beatings of counterpropagating waves in a Zeeman ring laser in a strong magnet field

A.S. Kudryavtsev, E.G. Lariontsev, I.I. Saveliev

*Abstract.* **We have theoretically and experimentally studied the regime of beatings of counterpropagating waves in a Zeeman ring laser under the action of strong fields of ring permanent magnets on the active medium. We have for the first time calculated and measured the dependences of the frequency bias and the intensity of counterpropagating waves of such a laser on the lasing frequency detuning relative to the frequency of the gain line centre. We have revealed some features in the dependence of the frequency bias on the magnetic field strength, associated with the nonlinearity of the active medium polarisability in strong inhomogeneous magnetic fields.**

***Keywords:*** *ring laser, laser gyroscope, frequency bias, Zeeman effect, magnetic field inhomogeneity.*

## 1. Introduction

Zeeman laser gyros are used in strapdown inertial navigation systems to obtain information about the rotation of objects moving in space with angular velocities varying over a wide range [1]. The dead zone near low angular velocities, despite the polarisation decoupling, is the main obstacle for improving accuracy in these and other types of laser gyros [2]. To get out of the dead zone, the Zeeman ring laser (ZRL) makes use of a frequency bias, which appears due to the Zeeman effect when a magnetic field is applied to the active medium [3, 4]. Usually, the magnetic field in a ZRL is formed using a solenoid. This leads to an increase in heat release in the ZRL and makes an additional contribution to the zero offset of its frequency response [5–7]. In addition, the reduction in losses in such lasers, which is necessary to lower nonreciprocal effects, causes a decrease in the frequency bias amplitude and complicates the solution of problems associated with the locking of counterpropagating waves. In using permanent magnets instead of a solenoid, one can reduce energy consumption and thermal drift, as well as increase the frequency bias due to the use of stronger magnetic fields [8, 9].

The aim of this work is to study theoretically and experimentally the region of existence of a two-frequency regime, as well as the intensities of counterpropagating waves and frequency bias obtained by the Zeeman effect in an active medium using a ring permanent magnet.

**A.S. Kudryavtsev, E.G. Lariontsev, I.I. Saveliev** OJSC M.F. Stel'makh Polyus Research Institute, ul. Vvedenskogo 3/1, 117342 Moscow, Russia; e-mail: bereg@niipolyus.ru, akudr-delta@yandex.ru

Received 1 July 2021; revision received 4 September 2021
*Kvantovaya Elektronika* **51** (11) 1004–1008 (2021)
Translated by M.A. Monastyrskiy

## 2. Experimental stand

The scheme of the experimental stand for studying the regime of beatings of counterpropagating waves is shown in Fig. 1. The stand consists of a personal computer (PC), an Ophir photodetector (PD300R model), an Espec MC-812 camera for dimming the ZRL, a test and monitoring device (PKI-6MT), and a K-5 type ZRL of our own production.

A two-frequency ZRL is installed in the Espec chamber to eliminate extraneous light when obtaining dependences of the wave intensity on the detuning. Ring permanent magnets are placed in the ZRL gas-discharge gaps to form frequency nonreciprocity in the laser active medium. A mixing prism and photodetectors are located on the ZRL plane mirror, which allow recording the beatings of counterpropagating waves. To measure the intensities $I_1$ and $I_2$ of counterpropagating waves, the Ophir photodetector is installed near the spherical mirror in position 1 to assess the intensity of a wave propagating counterclockwise, or in position 2 to evaluate the intensity of a wave propagating clockwise. The Ophir photodetector signals are fed directly to the PC and visualised by the Ophir StarLab software. Piezoelectric drivers allow one to vary the ZRL perimeter and thereby to detune the lasing frequency. The PKI-6MT ignites the discharge and monitors the currents in the gas-discharge gaps ($i_1$ and $i_2$), controls the voltage on the piezoelectric drivers ($U_{\text{piezo}}$), converts the analogue signals of the photodetectors into digital signals of the standard USB port of the PC, and transmits the digital data to the PC. The beating frequency of the counterpropagating waves and the voltage on the piezoelectric drivers were processed and recorded using the software developed at the Polyus Research Institute.

## 3. Results

To analyse the ZRL amplitude–frequency characteristics, we use the results of theoretical studies of this laser, presented in [10, 11]. For the complex amplitudes $E_{1,2}$ of the counterpropagating waves, we write the following system of ordinary differential equations:

$$\dot{E}_{1,2} = \frac{\Delta\nu}{2}\Big(\langle\kappa_{1,2}\rangle\frac{n}{n_0} - 1 - \langle\alpha_{1,2}\rangle\big|E_{1,2}\big|^2 - \langle\beta_{1,2}\rangle\big|E_{2,1}\big|^2\Big)E_{1,2}, \quad (1)$$

where $\Delta\nu$ is the resonator bandwidth; $\langle\kappa_{1,2}\rangle$, $\langle\alpha_{1,2}\rangle$, and $\langle\beta_{1,2}\rangle$ are the averaged coefficients describing the amplifying medium polarisability; $n$ is the relative excess of gain over losses at the gain line maximum; and $n_0$ is the value of $\langle\kappa_{1,2}\rangle$ at the gain line maximum. Let us consider the two-frequency regime when the fields $E_{1,2}$ of the counterpropagating waves correspond to a single longitudinal mode and are circularly polar-

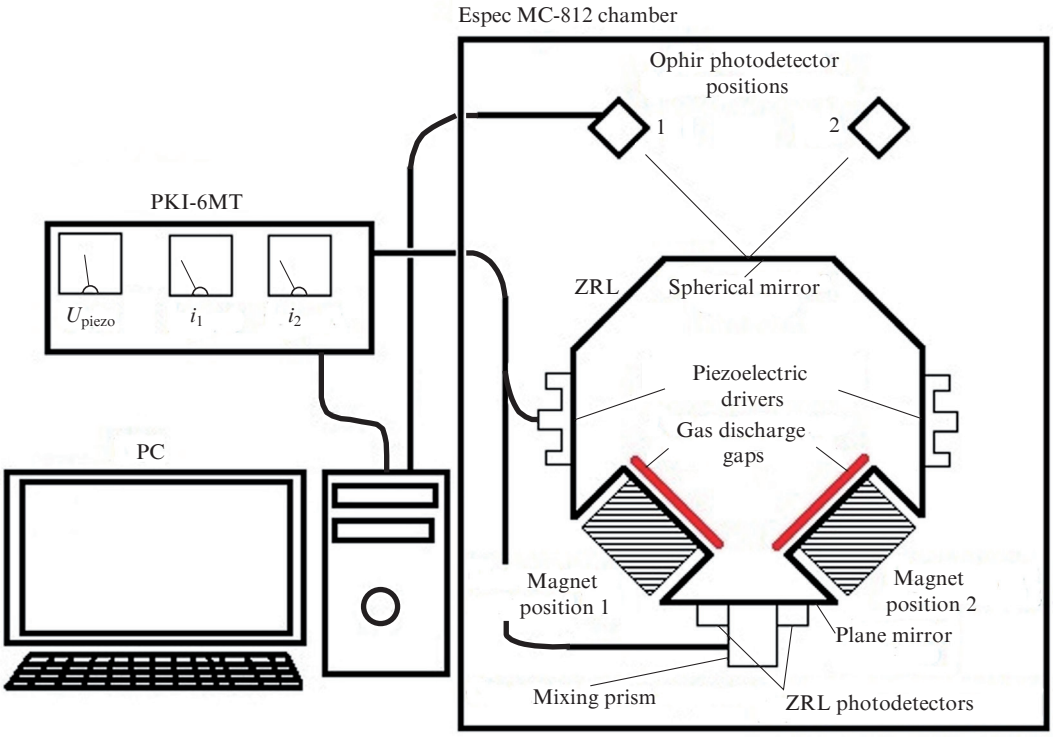


**Figure 1.** Schematic of the experimental stand.

ised. The amplitude of the frequency bias formed when a magnetic field is applied to the amplifying medium significantly exceeds the width of the lock-in region; therefore, the coupling of counterpropagating waves through backscattering is not taken into account in Eqns (1).

The authors of Refs [10, 11] presented formulas for the coefficients $\kappa_{1,2}$, $\alpha_{1,2}$, and $\beta_{1,2}$ describing the amplifying medium polarisability with allowance for the Zeeman effect in an external homogeneous longitudinal magnetic strength field $H$. Under the action of this field, the Zeeman splitting of the laser transition levels occurs,

$$\mu = g\beta H, \tag{2}$$

where $\beta$ is the Bohr magneton, and $g$ is the Landé $g$-factor.

When using a ring permanent magnet, the field $H$ on the laser beam axis is substantially inhomogeneous, up to a change in the sign of its strength, i. e. $H$ is a function of the coordinate $x$ along the axis of the ring resonator contour, $H = H(x)$, and, consequently, the Zeeman splitting is described by the function $\mu(x)$. The coefficients $\kappa_{1,2}$, $\alpha_{1,2}$, and $\beta_{1,2}$, depending on $\mu(x)$, also become the functions of the coordinate $x$: $\kappa_{1,2}(x)$, $\alpha_{1,2}(x)$, and $\beta_{1,2}(x)$. The coefficients $\langle\kappa_{1,2}\rangle$, $\langle\alpha_{1,2}\rangle$, and $\langle\beta_{1,2}\rangle$, included in Eqn (1) are calculated by averaging $\kappa_{1,2}(x)$, $\alpha_{1,2}(x)$, and $\beta_{1,2}(x)$ over the ring resonator region in which the gas discharge is burning. For example,

$$\langle\kappa_{1,2}\rangle = \frac{1}{L}\int_0^L \kappa_{1,2}(x)\,\mathrm{d}x,$$

where $L$ is the length of the region occupied by the discharge.

Let us consider the results of calculations based on the ZRL parameters used in the experiment. The ZRL on a single Ne isotope operated at a gas mixture pressure of 700 Pa. We assume that at the line centre the relative excess of the gain over loss is $n = 1.13$ with a loss value of 0.18%. The Landé $g$-factor is 1.2.

In the experiment, permanent AlNiCo-alloy magnets (YuNDK-15 magnets in positions 1 and 2) were used to generate a magnetic field (Fig. 1). Figure 2 shows the longitudinal magnetic field strength $H$ formed by a single ring magnet with a length of 9 mm (position 1) as a function of the coordinate $x$ along the optical contour axis. The field distribution on the ring magnet axis was measured using a TPU-01 milliteslameter. The gas discharge was burning in one half of the ring resonator contour. The length of the area occupied by the discharge was $L = 4.8$ cm.

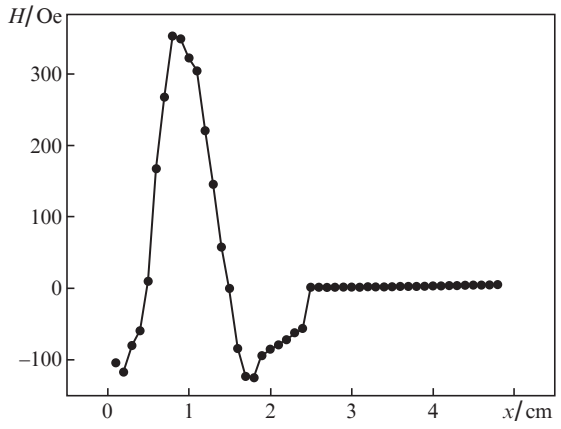


**Figure 2.** Magnetic field strength distribution in the gas discharge region.

As applied to this magnetic field strength distribution, Fig. 3 shows approximating (solid curves) and experimentally measured (points) dependences of the frequency bias $F_b$ on the lasing frequency detuning $\xi$ relative to the frequency of the gain line centre for two modes with opposite circular polarisations. The intra-resonator losses per round trip of the light in the resonator amounted to 0.18% for one of these modes (Fig. 3a), and 0.19% for the other (Fig. 3b).

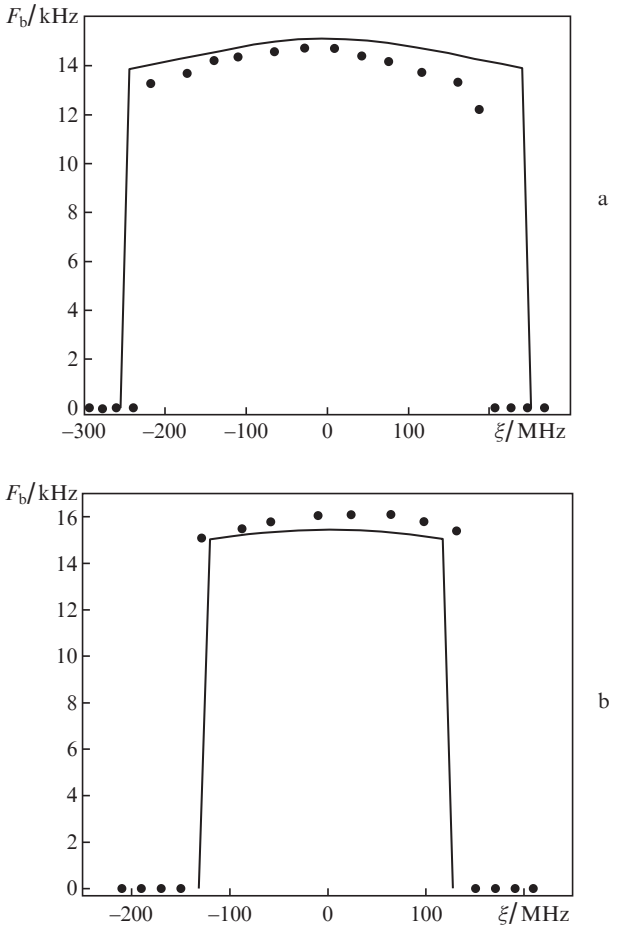


**Figure 3.** Dependences of the frequency bias on the lasing frequency detuning $\xi$ for modes with losses of (a) 0.18% and (b) 0.19%.

For the magnetic field distributions shown in Fig. 2, Fig. 4 presents the theoretical (solid curves) and experimentally measured (points) dependences of the normalised-to-unity intensities $I_1$ and $I_2$ for counterpropagating waves (dark and light points, respectively) on the lasing frequency detuning $\xi$ relative to the gain line centre for a single circularly polarised mode, with losses of 0.18% per single round trip for the light in the resonator.

Similar studies were performed using two permanent AlNiCo-alloy magnets (YuNDK-15 brand) located in positions 1 and 2 (Fig. 1). Figure 5 shows the experimental strength distribution for the longitudinal magnetic field $H(x)$ formed by such magnets with a length of 9 mm. The gas discharge was burning in one half of the ring resonator contour.

For this magnetic field strength distribution, Fig. 6 shows theoretical (solid curves) and experimentally measured (points) dependences of the frequency bias $F_b$ on the lasing frequency tuning $\xi$ relative to the gain line centre for two

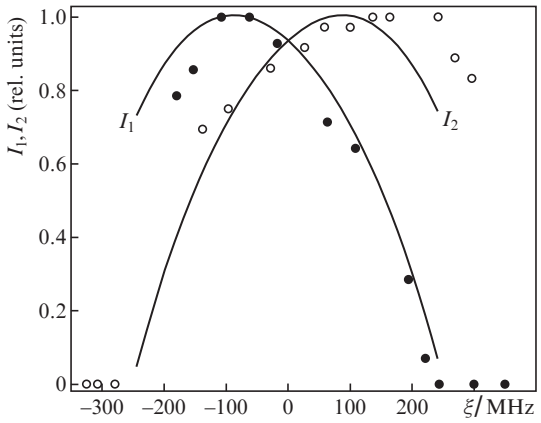


**Figure 4.** Dependence of the intensities $I_1$ and $I_2$ of the counterpropagating waves on the lasing frequency detuning $\xi$ for the mode with losses of 0.18%.

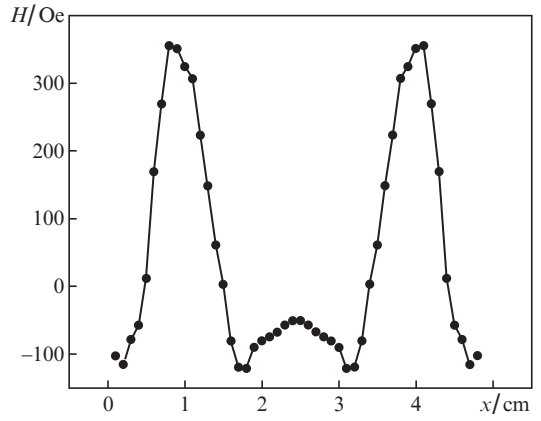


**Figure 5.** Distribution of the magnetic field strength of two permanent magnets (YuNDK-15 brand) in the gas discharge region.

modes with opposite circular polarisations. For these modes, the intra-resonator losses for a single round trip for the light in the resonator amounted to 0.18% (Fig. 6a) and 0.19% (Fig. 6b), respectively.

The ZRL frequency and amplitude characteristics in the regime of beatings of counterpropagating waves, presented in Figs. 3, 4, and 6, show that the experimental and theoretical results are in satisfactory quantitative agreement both in terms of the frequency bias magnitude, and the width of the region of lasing frequency detuning from the centre of the gain line in which the regime of beatings of counterpropagating waves is implemented.

The experimental studies presented in this work were performed using AlNiCo-alloy magnets (YuNDK-15 brand). There are magnets made of other materials, such as SmCo alloy, which are capable of generating stronger magnetic fields. Figure 7 shows the experimental distribution of the magnetic field strength generated by a single ring magnet 9 mm long made of the SmCo alloy (KS25DTs-225 brand) located in position 1 (Fig. 1). It was assumed that the SmCo-alloy magnet generates a field with a strength five times greater than that of the AlNiCo-alloy magnet.

Figure 8 shows the calculated dependence of the frequency bias $F_b$ on the lasing frequency detuning $\xi$ for this field

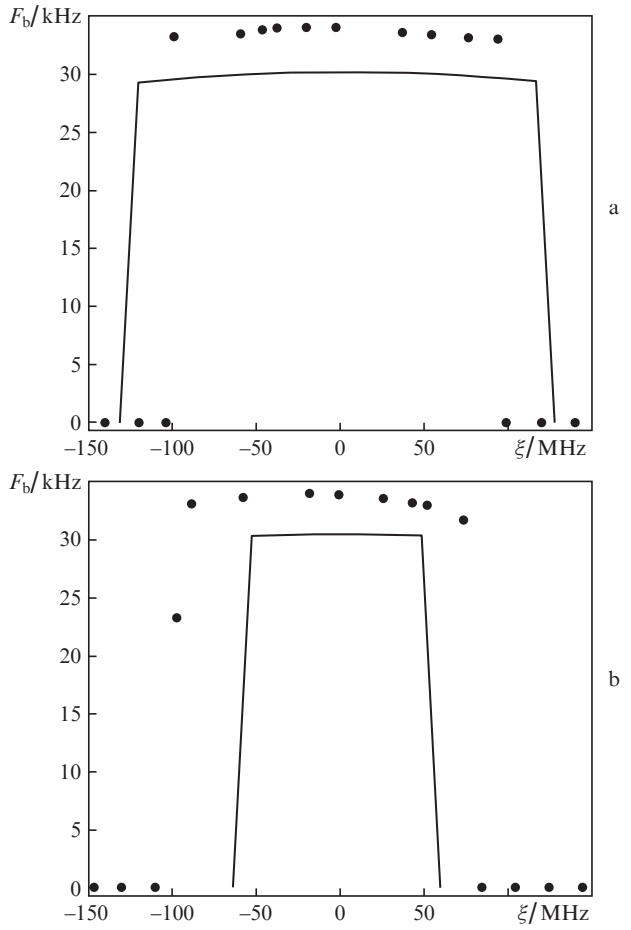


**Figure 6.** Dependences of the frequency bias formed by two AlNiCo-alloy magnets on the lasing frequency detuning $\xi$ for modes with losses of (a) 0.18% and (b) 0.19%.

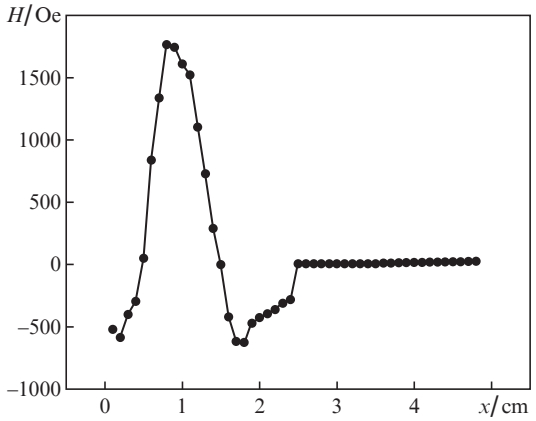


**Figure 7.** Magnetic field strength distribution of a permanent SmCo-alloy magnet in the gas discharge region.

strength distribution. The calculations assumed that the relative excess of the gain over losses at the line centre was $n = 1.4$, while losses in the resonator amounted to 0.18%.

One can see from Fig. 8 that the sign of the frequency bias changes in the case of a stronger magnetic field. Qualitatively, this can be explained as follows. The main contribution to the frequency bias is made by the coefficients $\langle\kappa_{1,2}\rangle$ describing the linear polarisability of the amplifying medium [10, 11]:

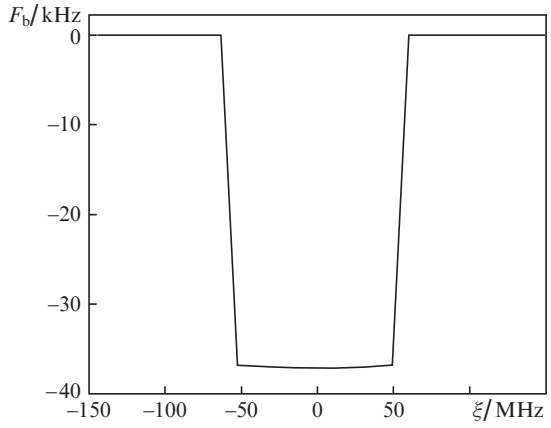


**Figure 8.** Dependence of the frequency bias formed by a SmCo-alloy magnet on the lasing frequency detuning $\xi$ for a mode with losses of 0.18%.

$$F_b = \frac{\Delta\nu}{2}\frac{n}{n_0}\left(\langle \mathrm{Im}\,\kappa_1\rangle - \langle \mathrm{Im}\,\kappa_2\rangle\right). \tag{3}$$

In the case of a homogeneous line width being small compared to the Doppler width $k_B u$, we can write an approximate expression for $\langle \mathrm{Im}\,\kappa_{1,2}\rangle$:

$$\langle \mathrm{Im}\,\kappa_1\rangle = -\langle \mathrm{Im}\,\kappa_2\rangle = \frac{1}{L}\int_0^L \left[\frac{2\mu(x)}{k_B u}\right] \times \exp\left\{-\left[\frac{\mu(x)}{k_B u}\right]^2\right\}\mathrm{d}x, \tag{4}$$

where $k_B$ is the Boltzmann constant, and $u$ is the average velocity of gas molecules. In the magnetic field distribution $H(x)$ there are regions with positive and negative values of the strength of the longitudinal magnetic field $H$. For the magnetic field strength distributions shown in Figs 2 and 5, the main contribution to the frequency bias $F_b$ is made by a region of positive $H$ values. On the contrary, for the field strength distribution in Fig. 7, due to the presence of the exponential factor $\exp\{-[\mu(x)/(k_B u)]^2\}$ in (4), the contribution of large positive $H$ values is significantly reduced, while the contribution of much smaller (in absolute magnitude) negative values dominates. As a result, the frequency bias changes its sign.

Thus, when a frequency bias is formed in the ZRL due to the Zeeman effect in inhomogeneous magnetic fields, there arises a feature associated with a significant decrease in the contribution of the regions of the strongest magnetic field, which undoubtedly requires experimental verification.

It should be noted that the theoretical aspects of this work took into account only the effect of the longitudinal magnetic field component (along the laser beam) on the active medium. The contribution of the transverse field component $H$ was neglected. It is possible that in the case of strong fields of magnets made of SmCo alloy, the contribution of the transverse field component will be significant. This issue requires further study.

## 4. Conclusions

We have studied theoretically and experimentally the frequency bias in the ZRL, which occurs due to the Zeeman effect when inhomogeneous magnetic fields generated by per-

manent magnets are applied to the amplifying medium. The dependence of the frequency bias value on the lasing frequency detuning from the gain line centre is investigated. A detuning region is found in which there exists the regime of beatings of counterpropagating waves. A feature has been revealed in the frequency bias dependence on the inhomogeneous field strength of the magnet, associated with a decrease in the contribution of the regions of the magnet's strongest field, which is due to the nonlinearity of the active medium polarisability. The results of experimental and theoretical studies of the ZRL amplitude–frequency characteristics are in satisfactory quantitative agreement.

## References


1. Luk'yanov D.P., Filatov Yu.V., Golyaev Yu.D., Kuryatov V.N., Vinogradov V.I., Schreiber K.-U., Perlmutter M. *Fotonika*, **1** (43), 42 (2014).
2. Rybakov B.V., Skulachenko S.S., Khromykh A.M., Yudin I.I. *Zh. Eksp. Teor. Fiz.*, **64**, 1146 (1973).
3. Azarova V.V., Golyaev Yu.D., Dmitriev V.G. *Quantum Electron.*, **30**, 96 (2000) [*Kvantovaya Elektron.*, **30**, 96 (2000)].
4. Azarova V.V., Golyaev Yu.D., Saveliev I.I. *Quantum Electron.*, **45**, 171 (2015) [*Kvantovaya Elektron.*, **45**, 171 (2015)].
5. Kolbas Yu.Yu., Grushin M.E., Gorshkov V.N. *Quantum Electron.*, **48**, 283 (2018) [*Kvantovaya Elektron.*, **48**, 283 (2018)].
6. Kudryavtsev A.S., Saveliev I.I., Savchenko N.A. *Collection of Abstracts of Competition Works of The 11th All-Russian Intersectoral Youth Competition of Scientific and Engineering Works and Projects "Youth and The Future of Aviation and Cosmonautics"* (Moscow: MAI Publisher, 2019).
7. Kudryavtsev A.S., Saveliev I.I., Savchenko N.A. *Proceedings of The Conference-Competition for Young Physicists* (Moscow: MFO Publishing House, 2019) Vol. 25, No. 2C.
8. Kudryavtsev A.S., Saveliev I.I., Savchenko N.A. *Trudy MAI*, (111), 18 (2020).
9. Saveliev I.I., Kudryavtsev A.S. Patent of the Russian Federation 2688952C1. Priority date 12.11.18.
10. Khromykh A.M., Yakushev A.I. *Sov. J. Quantum Electron.*, **7**, 13 (1977) [*Kvantovaya Elektron.*, **4**, 27 (1977)].
11. Savel'ev I.I., Khromykh A.M., Yakushev A.I. *Sov. J. Quantum Electron.*, **9**, 682 (1979) [*Quantum Electron.*, **6**, 1155 (1979)].